Enabling Extremely High Dynamic Range Measurements using a Simple Correlator

Brett T. Walkenhorst
NSI-MI Technologies
Suwanee, GA 30024
bwalkenhorst@nsi-mi.com

***Abstract*—In order to achieve high accuracy in measuring sidelobes and/or nulls in antenna patterns, it is necessary to use a test system with very high dynamic range. This is particularly important when the antenna has extremely high gain such as those used for certain satellite communications or radio astronomy applications or when transmit power is limited relative to range loss as is often the case in millimeter wave applications. For several years, commercially available antenna measurement receivers have offered a dynamic range as high as 135dB for such applications. This dynamic range has been made possible, in part, by a simple correlator in the receiver's DSP chain. In this paper, we model the various sources of error in a test signal due to imperfections and uncertainties of the test equipment and the physical environment and analyze these models as they propagate through the receive chain. The results of that analysis demonstrate the correlator's ability to reduce carrier frequency offset (CFO) and local oscillator (LO) phase noise to offer the fidelity of test signal necessary to achieve extremely high dynamic ranges of up to 135dB.**

***Index Terms*—High Dynamic Range, Antenna Measurement Receiver, Correlator**

I. Introduction

In certain antenna measurement applications, high dynamic range is an important requirement. In designing a broadband receiver system to meet these requirements, there are several architectural elements that play important roles. The purpose of this paper is to highlight and analyze one of these critical components, a fairly simple DSP process known as a single sample correlator.

The analysis that follows is based on the architecture of the MI-750 Receiver from NSI-MI Technologies. While the MI-750 Receiver is used as a representative architecture to illustrate the concept of the correlator, an analysis of other receiver architectures would likely yield similar results.

A. Dynamic Range

Dynamic range is defined as the ratio of the largest to the smallest values of a measurable quantity [1]. Applied to a measurement receiver, dynamic range is a metric of the range of amplitudes the receiver can reliably measure. Assuming other potential dynamic range bottlenecks are not a limiting factor, such as A/D quantization, spurious free dynamic range, intermodulation distortion, etc., then the dynamic range of the receiver is fundamentally limited by the thermal noise power, which is given by [1]

$$P_n = k_B T_0 B F_N \quad (1)$$

where P_n is the noise power, k_B is Boltzmann's constant, T_0 is the temperature of the system, B is the noise bandwidth, and F_N is the receiver's noise factor.

The MI-750 Receiver has selectable IF sample rates. The choice of sample rate sets the bandwidth of the noise seen by the receiver. The lower the sample rate, the lower the noise power and the higher the dynamic range [2] as illustrated in Figure 1. At its lowest sample rate setting of 1Hz, the difference between the MI-750 Receiver's maximum RF receive power and the thermal noise power given by (1) is 135dB.

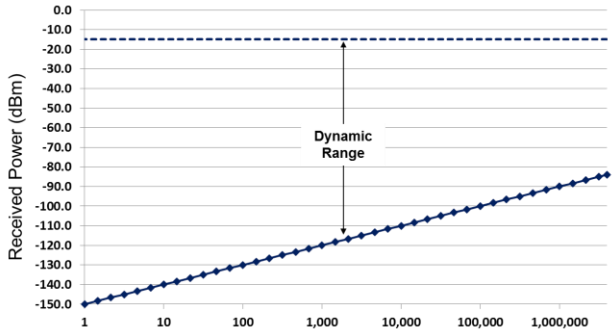

Figure 1. Illustration of Receiver Dynamic Range vs. Sample Rate

Unfortunately, other considerations such as carrier frequency offset (CFO) and phase noise can prevent such low rate measurements from yielding reliable results. The purpose of the correlator, as will be seen in Section IV, is to mitigate these limiting factors and enable low sample rate, high dynamic range measurements.

B. System Architecture

The relevant components of the receiver architecture are depicted in Figure 5, a somewhat simplified architectural view of the MI-750 Receiver [3].

Following the flow of Figure 5, in Section II, we will model the transmit signals: $x_A(t)$ and $x_R(t)$; and the channels: $h_A(t)$, $h_R(t)$, $h_{LO,A}(t)$, and $h_{LO,R}(t)$; and in Section III, we model the local oscillator (LO) signal: $y_{LO}(t)$; and the received signals at various stages of processing: $y_A(t)$, $y_R(t)$, $y_A^B(t)$, $y_R^B(t)$, $y_A^C(t)$, $y_R^C(t)$, $y_{AR}(t)$, and $y_{AR}^C(t)$.

The signal source, coupler, antennas, cables, mixers, correlator, and divider are all explicitly modeled. The other elements including diplexers, A/D converters, and digital filters are included in the diagram to aid the reader's understanding of some parts of the model development, but are not explicitly modeled. The A/D converters and digital decimating filters, however, are treated in some detail in

Section IV to describe the impact of the correlator. Section IV also contains general observations on the analysis including a brief treatment of some common antenna measurements based on the paper's mathematical models. Conclusions are presented in Section V.

II. Signal and Channel Models

A. Transmit Signal Model

The transmit signal is modeled as [4]

$$x_A(t) = \sqrt{P_T} e^{j(\omega_T t + \phi_T(t) + \phi_{T_0})} \tag{2}$$

where P_T is the transmit signal power, $\omega_T = \omega_c + \omega_{T_\Delta}$ is the transmit frequency, ω_c is the intended carrier frequency, ω_{T_Δ} is the frequency offset due to an unstable and/or frequency resolution limited transmit clock, $\phi_T(t)$ is a time-dependent phase term representing phase noise on the transmit clock, and ϕ_{T_0} is an absolute unknown phase offset.

The signal sent to the reference cable is coupled off the main line at a reduced power, perhaps 10 to 20dB down depending on the coupler that is used. This reduction is modeled as

$$x_R(t) = \alpha x_A(t) \tag{3}$$

where $0 < \alpha < 1$.

B. Channel Models

For this analysis, the channel over the air is modeled as a delta function, which is defined as zero everywhere except when the argument of the function is zero. This model assumes the environment is a pristine chamber with no multipath. The model is given by

$$h_A(t) = \kappa_A \kappa_P \frac{e^{-jkr}}{2kr} \delta(t - t_A) \tag{4}$$

where κ_A and κ_P are complex (i.e. magnitude and phase) responses of the AUT and Probe antenna respectively, r is the over-the-air distance, $k = 2\pi/\lambda$ is the wave number associated with the transmit frequency where $\lambda = \frac{c}{\omega_T/2\pi}$, and $t_A = r/c$ is the time it takes the EM wave to cross the air gap. The antenna responses are actually functions of the transmit frequency and antenna pointing angle, i.e. $\kappa_A = \kappa_A(f_T, \theta_A, \phi_A)$ and $\kappa_P = \kappa_P(f_T, \theta_P, \phi_P)$, but for brevity, we omit these parameters.

The channel of the reference cable is also modeled as a delta function,

$$h_R(t) = \beta \delta(t - t_R) \tag{5}$$

where $\beta \leq 1$ is the square root of the power loss through the cable and t_R is the temporal delay due to the cable.

The signal LO cable channel is modeled as

$$h_{LO,A}(t) = \beta_A \delta\left(t - t_{LO,A}\right) \tag{6}$$

and the reference LO cable channel as

$$h_{LO,R}(t) = \beta_R \delta\left(t - t_{LO,R}\right). \tag{7}$$

C. Noiseless Received Signal Models

In this paper, we limit our analysis to the noiseless case. Assuming no noise, the signal received over the air is given by

$$y_A(t) = h_A(t) * x_A(t) \tag{8}$$

Using (2) and (4), we write the received signal as

$$\begin{aligned} y_A(t) &= \kappa_A \kappa_P \frac{e^{-jkr}}{2kr} x_A(t - t_A) \\ &= \kappa_A \kappa_P \frac{\sqrt{P_T}}{2kr} e^{j\left(\omega_T t + \phi_T(t - t_A) + \left(\phi_{T_0} - \omega_T t_A - kr\right)\right)} \end{aligned} \tag{9}$$

Using (3) and (4), we write the received reference signal as

$$\begin{aligned} y_R(t) = h_R(t) * x_R(t) &= \alpha\beta x_A(t - t_R) \\ &= \alpha\beta \sqrt{P_T} e^{j(\omega_T t + \phi_T(t - t_R) + \phi_{T_0} - \omega_T t_R)} \end{aligned} \tag{10}$$

III. Digital Signal Processing

A. Conversion to Complex Baseband

In the receiver, we mix both signal and reference channels down to complex baseband. The configuration depicted in Figure 5 shows an external analog mixing stage followed by a complex digital mixing stage, but we will model a single mixer as the combination of these two stages and, for convenience, we will preserve the continuous-time notation for now. The LO signal is given by

$$y_{LO}(t) = e^{-j(\omega_R t + \phi_R(t) + \phi_{R_0})} \tag{11}$$

where $\omega_R = \omega_c + \omega_{R_\Delta}$ is the frequency of the LO signal, ω_{R_Δ} is the LO's CFO, $\phi_R(t)$ is the LO's phase noise, and ϕ_{R_0} is the LO's absolute phase offset.

If we assume the LO power is sufficient for the mixer to operate properly, we can assume the conversion loss is invariant to the LO power and ignore the loss of the cable applied to the LO signal. We therefore let β_M represent the conversion loss of the mixer and write the complex baseband signal as

$$\begin{aligned} y_A^B(t) &= \beta_M y_A(t) y_{LO}\left(t - t_{LO,A}\right) * h_{LO,A}(t) \\ &= \kappa_A \kappa_P \frac{\beta_M \beta_A \sqrt{P_T}}{2kr} e^{j\xi_{AB}(t)} \end{aligned} \tag{12}$$

where

$$\begin{aligned} \xi_{AB}(t) = \omega_{CFO} t &+ \phi_T\left(t - t_A - t_{LO,A}\right) \\ &- \phi_R\left(t - 2t_{LO,A}\right) \\ &+ (\omega_R - \omega_{CFO}) t_{LO,A} + \phi_{T_0} - \omega_T t_A \\ &- \phi_{R_0} - kr \end{aligned} \tag{13}$$

is a complicated phase function including CFO, phase noise, and phase offset and

$$\omega_{CFO} = \omega_T - \omega_R = \omega_{T_\Delta} - \omega_{R_\Delta} \tag{14}$$

is the baseband CFO.

The baseband representation of the reference signal is given by

$$y_R^B(t) = \beta_M y_R(t) y_{LO}\left(t - t_{LO,R}\right) * h_{LO,R}(t) = \alpha\beta_M\beta\beta_R\sqrt{P_T}e^{j\xi_{RB}(t)} \quad (15)$$

with a similarly complicated phase term given by

$$\xi_{RB}(t) = \omega_{CFO}t + \phi_T\left(t - t_R - t_{LO,R}\right) - \phi_R\left(t - 2t_{LO,R}\right) + (\omega_R - \omega_{CFO})t_{LO,R} + \phi_{T_0} - \omega_T t_R - \phi_{R_0}. \quad (16)$$

B. Correlator

In order to compare performance to a baseline, we will consider the results with the correlator on as well as off. The correlator simply conjugates the reference and multiplies it by the signal received over the air. The post-correlated signal is given by

$$y_A^C(t) = y_A^B(t)y_R^{B^*}(t) = \kappa_A\kappa_P\frac{\alpha\beta_M^2\beta\beta_A\beta_R P_T}{2kr}e^{j\xi_{AC}(t)} \quad (17)$$

where

$$\xi_{AC}(t) = \phi_T\left(t - t_A - t_{LO,A}\right) - \phi_T\left(t - t_R - t_{LO,R}\right) + \phi_R\left(t - 2t_{LO,R}\right) - \phi_R\left(t - 2t_{LO,A}\right) + (\omega_R - \omega_{CFO})\left(t_{LO,A} - t_{LO,R}\right) + \omega_T(t_R - t_A) - kr. \quad (18)$$

Notice the CFO has disappeared. While ω_{CFO} is still in the phase term, it does not multiply the time variable; it therefore contributes to an absolute phase offset, but has no effect on the frequency. Under some simplifying assumptions discussed below, the phase noise terms will also disappear.

The correlator also correlates the reference with itself, so the post-correlated reference channel yields a real-valued signal given by

$$y_R^C(t) = y_R^B(t)y_R^{B^*}(t) = \alpha^2\beta_M^2\beta^2\beta_R^2 P_T. \quad (19)$$

C. Signal Divided by Reference (A/R) with Correlator On

With the correlator on, the A/R signal is computed by dividing the post-correlated signal channel by the post-correlated reference channel:

$$y_{AR}^C(t) = \frac{y_A^C(t)}{y_R^C(t)} = \kappa_A\kappa_P\frac{\beta_A}{2kr\alpha\beta\beta_R}e^{j\xi_{AC}(t)}. \quad (20)$$

At this point, the CFO has been eliminated, but we have some phase noise terms remaining. We can simplify this further if we make some assumptions about the phase noise. To simplify notation, we assume $\phi_T(t)$ and $\phi_R(t)$ are wide sense stationary, meaning the statistics of the phase noise terms are independent of time, but this is not strictly necessary.

1) Assumption #1: Transmitter phase noise is negligible

The auto-correlation function of the transmit phase noise is given by $\rho_T(\tau) \equiv E[\phi_T(t)\phi_T^*(t-\tau)]$. If the correlation between $\phi_T\left(t - t_A - t_{LO,A}\right)$ and $\phi_T\left(t - t_R - t_{LO,A}\right)$ is sufficiently high, i.e.

$$\rho_T\left(t_R + t_{LO,R} - \left(t_A + t_{LO,A}\right)\right) \approx \rho_T(0) \quad (21)$$

then

$$\phi_T\left(t - t_A - t_{LO,A}\right) - \phi_T\left(t - t_R - t_{LO,R}\right) \approx 0 \quad (22)$$

This implies that the spectral width of the transmit signal is small relative to the inverse of the differential time $t_R + t_{LO,R} - \left(t_A + t_{LO,A}\right)$. This may be achieved by some combination of a low phase noise transmitter (narrower spectrum) and matching the delay of the main signal channel (h_A and $h_{LO,A}$) to the delay of the reference signal channel (h_R and $h_{LO,R}$).

2) Assumption #2: Receiver LO phase noise is negligible

With correlation of receive phase noise defined similarly, if

$$\rho_R\left(2t_{LO,A} - 2t_{LO,R}\right) \approx \rho_R(0) \quad (23)$$

then

$$\phi_R\left(t - 2t_{LO,R}\right) - \phi_R\left(t - 2t_{LO,A}\right) \approx 0 \quad (24)$$

As with the first assumption, this may be achieved by some combination of low phase noise on the receiver's LO and matching the delay of the post-mixer cables for the signal ($h_{LO,A}$) and reference ($h_{LO,R}$) channels.

3) Simplified Expression

Using the assumptions above, we can simplify the equation for the noise-free A/R calculation with the correlator on by the approximation

$$y_{AR}^C(t) \approx \kappa_A\kappa_P\frac{\beta_A}{2kr\alpha\beta\beta_R}e^{j\xi_{AR}} \quad (25)$$

where

$$\xi_{AR} = (\omega_R - \omega_{CFO})\left(t_{LO,A} - t_{LO,R}\right) + \omega_T(t_R - t_A) - kr \quad (26)$$

Notice the simplified expression for $y_{AR}^C(t)$ has no time component, so we can write it as y_{AR}^C or, if we like, we can introduce the angular parameters we omitted previously and write

$$y_{AR}^C(\theta,\phi) \approx \kappa_A(\theta,\phi)\kappa_P\left(\theta_P,\phi_P\right)\frac{\beta_A}{2kr\alpha\beta\beta_R}e^{j\xi_{AR}} \quad (27)$$

With the disappearance of the time component, the value measured as y_{AR} is simply a complex number. This assumes, of course, that we have met the phase noise and/or cable delay constraints described above. To the extent that the constraints are not met, any residual phase noise terms will have a time dependency and may be treated as noise. The extent to which this approximation is not valid and its impact on measurement fidelity is beyond the scope of this paper, but will be addressed in future work.

D. Signal Divided by Reference (A/R) with Correlator Off

With the correlator off, the A/R signal is given by

$$y_{AR}(t) = \frac{y_A^B(t)}{y_R^B(t)} = \kappa_A\kappa_P\frac{\beta_A}{2kr\alpha\beta\beta_R}e^{j\xi_{AC}(t)} \quad (28)$$

As before, if (21) and (23) hold, then we can approximate the noise-free A/R computation with the correlator off as

$$y_{AR}(t) \approx \kappa_A \kappa_P \frac{\beta_A}{2kr\alpha\beta\beta_R} e^{j\xi_{AR}} \quad (29)$$

IV. Observations

A. Impact of Correlator

Notice the noise-free A/R equations for the correlator on (25) and off (29) are identical, which should not be surprising considering

$$y_{AR}(t) = \frac{y_A^B(t)}{y_R^B(t)} = \frac{y_A^B(t)y_R^{B^*}(t)}{y_R^B(t)y_R^{B^*}(t)} = \frac{y_A^C(t)}{y_R^C(t)} = y_{AR}^C(t) \quad (30)$$

But there is a difference in their impact due to the sample rate at which the computations are made.

We haven't explicitly modeled the sample rates and decimating filters of the IF processor, but consider the generic baseband signal model in (12). There are two terms in the phase of that equation (13) that contribute to the frequency content of the signal that will be described below.

1) CFO

The first term from (13), $\omega_{CFO}t$, is the baseband CFO. From (14), $\omega_{CFO} = \omega_{T_\Delta} - \omega_{R_\Delta}$ indicating its dependence on both transmitter and receiver LO CFO terms. This term shifts the baseband frequency away from zero rad/sec. If our receiver clock was perfectly matched to the source clock, this term would go to zero; however, this may not be feasible in a practical system.

2) Phase Noise

The second term from (13), $\phi_T(t - t_A - t_{LO,A}) - \phi_R(t - 2t_{LO,A})$, is due to phase noise on the transmitter and LO signal. We can minimize this term by using extremely accurate, low phase noise oscillators, but sources such as this can be quite expensive and making them broadband is very difficult.

These two terms, CFO and phase noise, affect the frequency and bandwidth of the signal. When the correlator is on, the CFO and phase noise are eliminated by the correlator. When it is off, they are eliminated by the A/R computation. The difference between these cases is the sample rate at which the frequency terms are eliminated.

To keep the notation relatively simple, we have modeled the signals in continuous time, but in reality, they are discrete time relative to a certain sample rate, i.e. $y_A^B[n](f_s) = y_A^B(t)|_{t=n/f_s}$. As frequencies of the continuous time models begin to fall outside the first Nyquist zone for each successively lower sample rate in the DSP chain, they are filtered out by the decimating filters.

Let ω_ϕ denote the one-sided radial bandwidth induced by the differential phase noise. For sample rates that are low relative to the CFO (ω_{CFO}) plus phase noise bandwidth (ω_ϕ), we begin to lose signal power. If half the sample rate is less than the CFO minus the one-sided phase noise BW, then we lose the signal completely. In other words, if

$$\frac{f_s}{2} < \frac{1}{2\pi}\left(|\omega_{CFO}| - |\omega_\phi|\right) \quad (31)$$

then the signal will be entirely outside the IF passband and our A/R calculation will yield pure noise. A notional example of this is illustrated in Figures 2-4. In Figure 2, a signal with CFO and phase noise is shown with a fairly large IF passband. The signal, shown as a broad bump on the right side of the spectrum, will pass through the IF filter and the resulting A/R measurements will be relatively uncorrupted. The peak of the signal is off center due to CFO and the energy is broad due to phase noise spreading.

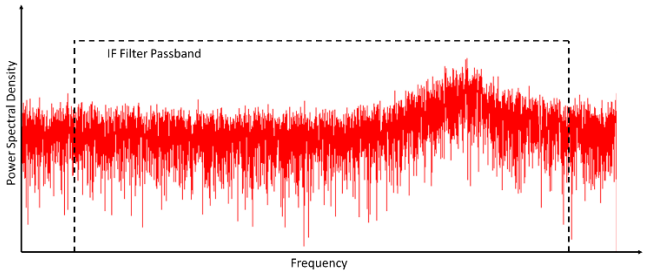

Figure 2. Power spectral density of notional signal with CFO and phase noise at high sample rate

In Figure 3, the same signal is shown with a lower sample rate. In this case, the CFO is sufficiently high that the signal falls outside the IF passband and will be filtered out before the A/R computation takes place.

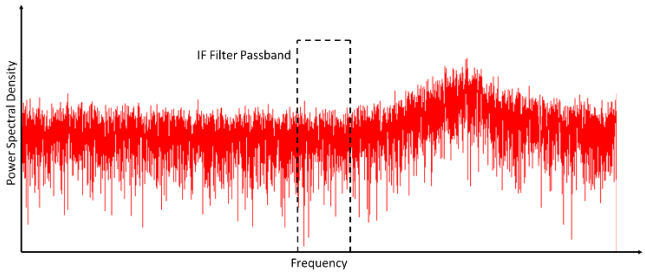

Figure 3. Power spectral density of notional signal with CFO and phase noise at low sample rate

In Figure 4, the signal has been centered and de-spread by the correlator such that its energy is captured in the narrower IF passband of the lower sample rate.

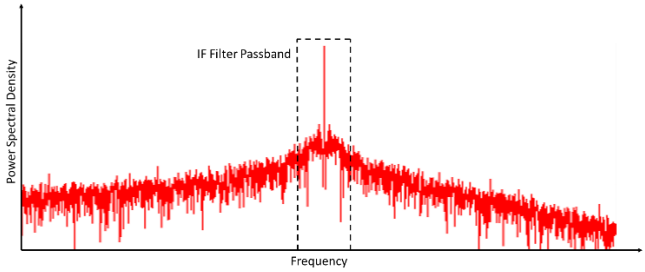

Figure 4. Power spectral density of post-correlated notional signal at low sample rate

In the MI-750 Receiver, the correlator occurs at a sample rate of 1.95Mcsps. For reasonably accurate clocks, the CFO

and phase noise should be well below this rate, i.e. $\frac{1}{2\pi}\left(|\omega_{CFO}| + |\omega_{\phi}|\right) \ll \frac{1.95e6}{2}$. Without the correlator, however, the A/R computation occurs at whatever output sample rate is chosen. If that sample rate meets the constraint in (31), then the signal will have been filtered out by one of the decimating filters before it ever gets to that sample rate. By removing the CFO and phase noise using the correlator, we center and de-spread the transmitted CW tone at a higher sample rate so that the lower sample rates will be assured of having signal present in the first Nyquist zone.

In summary, both the correlator and the computation of A/R eliminate the effect of CFO and phase noise, but for very low sample rates, the correlator is usually necessary to ensure we have signal in the final result.

B. Signal Model Applied to Practical Measurements

Note that the A/R measurements of (25) and (29) still contain a large number of unknowns, e.g. κ_P, β_A, r, α, β, β_R, ω_R, ω_T, $t_{LO,A}$, $t_{LO,R}$, t_R, and t_A. While some of these unknowns can be measured (e.g. r, α, β, etc) and some are known to some level of accuracy *a priori* (e.g. ω_R and ω_T), none are known exactly. Rather than attempt to directly measure each quantity and deal with the uncertainty and potential drift of all of these parameters, common antenna measurement techniques typically find ways of eliminating the unknowns.

In this section, we briefly consider the impact of these unknowns on three practical measurements within the context of the signal models developed above and show how the unknowns become irrelevant when handled properly. Other measurements can likewise be shown to eliminate the problems of the unknown parameters, but due to space constraints, we offer three examples to illustrate the basic concepts.

1) Antenna Patterns

When we wish to find the radiation pattern of the AUT, one of the simpler measurements we often conduct, we will compute the received signal as a function of pointing angle relative to the peak:

$$\begin{aligned} R(\theta,\phi) &= \frac{|y_{AR}(\theta,\phi)|}{\max\limits_{\theta,\phi}|y_{AR}(\theta,\phi)|} \\ &= \frac{|\kappa_A(\theta,\phi)|\left|\kappa_P(\theta_P,\phi_P)\frac{\beta_A}{2kr\alpha\beta\beta_R}\right|}{\max\limits_{\theta,\phi}|\kappa_A(\theta,\phi)|\left|\kappa_P(\theta_P,\phi_P)\frac{\beta_A}{2kr\alpha\beta\beta_R}\right|} \\ &= \frac{|\kappa_A(\theta,\phi)|}{\max\limits_{\theta,\phi}|\kappa_A(\theta,\phi)|} \end{aligned} \tag{32}$$

When computing a normalized pattern, all of the unknown parameters, e.g. κ_P, β_A, r, α, etc., disappear.

2) Gain by Substitution

It is the presence of these unknowns that makes direct antenna gain measurements more challenging than they might first appear. Antenna gains are functions of the antenna responses, $G_A = \max\limits_{\theta,\phi}|\kappa_A(\theta,\phi)|$ and $G_P = \max\limits_{\theta,\phi}|\kappa_P(\theta,\phi)|$. The simplest method of gain measurement uses a trusted gain standard to calibrate for these unknown parameters. Assuming we have an AUT where $G_{A'}$ is known, then we measure A/R (25) and find the maximum response over all angles:

$$\begin{aligned} y_{SGH} &= \max_{\theta,\phi}|y'_{AR}(\theta,\phi)| \\ &= \max_{\theta,\phi}|\kappa_{A'}(\theta,\phi)|\left|\kappa_P\frac{\beta_A}{2kr\alpha\beta\beta_R}\right| \\ &= G_{A'}\kappa_P\frac{\beta_A}{2kr\alpha\beta\beta_R} \end{aligned} \tag{33}$$

We then measure the unknown AUT in a similar manner:

$$\begin{aligned} y_{AUT} &= \max_{\theta,\phi}|y_{AR}(\theta,\phi)| \\ &= \max_{\theta,\phi}|\kappa_A(\theta,\phi)|\left|\kappa_P\frac{\beta_A}{2kr\alpha\beta\beta_R}\right| \\ &= G_A\kappa_P\frac{\beta_A}{2kr\alpha\beta\beta_R} \end{aligned} \tag{34}$$

and then compute

$$\frac{y_{AUT}}{y_{SGH}}G_{A'} = \frac{G_A\kappa_P\frac{\beta_A}{2kr\alpha\beta\beta_R}}{G_{A'}\kappa_P\frac{\beta_A}{2kr\alpha\beta\beta_R}}G_{A'} = G_A \tag{35}$$

which eliminates the unknown variables, κ_P, β_A, etc., since they appear in both the numerator and denominator of (35).

3) Near-field to Far-field Transform

Unlike the previous two measurement examples, which quickly eliminated the unknown phase ξ_{AR} by computing the magnitude of the measured response, a near-field to far-field transform requires precise phase information of the measured data. Write the A/R measurement as

$$y_{AR}(x,y,z) \approx \kappa_A(\theta,\phi)\kappa_P(\theta_P,\phi_P)\frac{\beta_A}{2kr\alpha\beta\beta_R}e^{j\xi_{AR}} \tag{36}$$

noting that θ, ϕ, θ_P, and ϕ_P are all functions of the probe position (x, y, z).

Although some manipulation may be done depending on the coordinate system used for the transformation, the essence of the near- to far-field transform is a spatial Fourier transform. Except for the probe response and the distance, r, all of the unknowns are spatially invariant. To the extent that r varies, it slightly modifies the magnitude of the measured near-field and effectively serves as a window function before transformation. Thus, we can treat the nominal distance as spatially invariant and lump all spatial variations into the transform. As all other variables are constant with respect to the spatial dimension, we can bring them outside the transform and, assuming we have done probe correction properly, write

$$y_{FF}(\theta,\phi) = \kappa_{A,FF}(\theta,\phi)\frac{\beta_A}{2kr\alpha\beta\beta_R}e^{j\xi_{AR}} \tag{37}$$

From this point, we are most likely interested in something like the far-field pattern, gain, etc. and will end up doing

magnitude-only computations similar to those described above, which will eliminate the unknown variables.

V. Conclusion

We have analyzed the effect of a simple correlator and demonstrated its ability to enable high dynamic range measurements by minimizing CFO and phase noise at a higher sample rate than the final IF rate. The analysis assumed the receiver experiences no thermal noise. Future work will report on the impact of thermal noise on the correlator's function. Future work will also address the impact of phase noise when the assumptions that allow us to neglect those terms are not sufficiently met.

Acknowledgment

The author gratefully acknowledges Steve Nichols, David Musser, and James Sakalaukus for sharing their knowledge of the MI-750 Receiver architecture.

References

[1] G. Gonzalez, "Microwave transistor amplifiers: analysis and design," *Prentice-Hall*, 1997.

[2] S. Nichols, "Advanced antenna measurement system architectures," *AMTA Symposium*, Nov 2011.

[3] NSI-MI Technologies, "MI-750 advanced digital receiver," MI-750 datasheet.

[4] IEEE 1139-2008, "IEEE standard definitions of physical quantities for fundamental frequency and time metrology – random instabilities," pp. 1-35, Feb 2009.

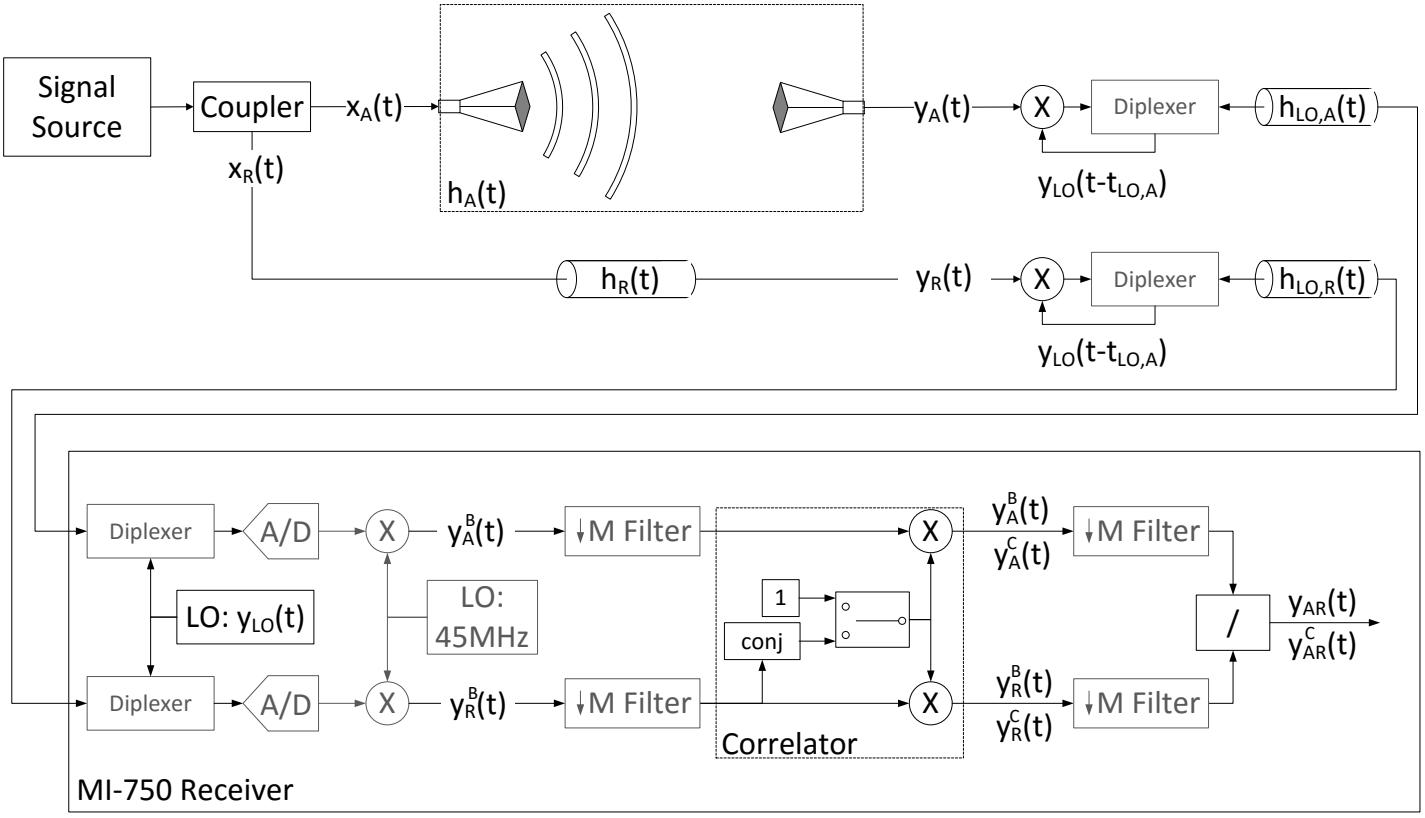

Figure 5. Simplified Antenna Measurement System Architecture